Available online on 15.08.2019 at http://jddtonline.info

Journal of Drug Delivery and Therapeutics

Open Access to Pharmaceutical and Medical Research

Open Access Research Article

Development and Evaluation of Nanoparticles Based Transdermal Patch of Agomelatine for the Treatment of Depression

Mahesh Shinde, Pramod Salve*, Shahadev Rathod

University Department of Pharmaceutical Sciences, Rashtrasant Tukadoji Maharaj Nagpur University, Nagpur (M.S.), India-440 033

ABSTRACT

Agomelatine (AGM) is an antidepressant drug. Its extensive hepatic first-pass metabolism coupled with low biological half-life shows 5% absolute bioavailability on oral administration. Polymeric nanoparticles (PNPs) have capability to efficiently penetrate the skin barrier and BBB so as to effectively reach the drug to site of action. Polymeric nanoparticles of drug (AGM-PNPs) with PLGA polymer were prepared by nanoprecipitation method followed by solvent evaporation. The particle size, polydispersity index, zeta potential and % entrapment efficiency of the optimized formulation were found to be compliant with the desired standards. DSC, FT-IR and XRD methods of instrumental analysis confirmed the formation of AGM-PNPs. Matrix–type transdermal patch containing AGM-PNPs (formulation TP 2) and AGM (formulation TP 1) were prepared by a solvent evaporation method using a film former machine. *In-vitro* drug release from patch formulations TP1 and TP2 were found to be 47.41 ± 1.78 and 70.16 ± 1.74. The drug release data of the *in-vitro* drug release study was analysed with kinetic models zero order, first order release kinetic model, Higuchi model, Korsmeyer-peppas model. In *ex-vivo* skin permeation studies, transdermal patch formulation containing AGMPNPs (TP 2) shown least lag time as compared to transdermal patch containing agomelatine (TP-1).

Article Info: Received 11 June 2019; Review Completed 18 July 2019; Accepted 26 July 2019; Available online 15 August 2019

Cite this article as:

Shinde M, Salve P, Rathod, Development and Evaluation of Nanoparticles Based Transdermal Patch of Agomelatine for the Treatment of Depression, Journal of Drug Delivery and Therapeutics. 2019; 9(4-s):126-144
http://dx.doi.org/10.22270/jddt.v9i4-s.3229

***Address for Correspondence:**

Dr. Pramod S. Salve, Associate Professor, University Department of Pharmaceutical Sciences, Rashtrasant Tukadoji Maharaj Nagpur University, Nagpur (M.S.), India - 440033

INTRODUCTION

Depression is a neuronal disorder with symptoms of reduced mood, lack of interest in day today life, low energy, low confidence in behavior, feelings of wrongdoing, poor concentration. It has affected about 350 million people in the world. As per the report of the world mental health survey conducted in 17 countries, 1 in 20 people has been found to suffer from depressive episodes last year. Anxiety is the common symptom often associated with depression and is the leading cause for suicidal tendencies leading to 1 million deaths annually. It has been observed that both genders are susceptible to depressive episodes but females are more prone to the development of depression than males **(Marcus *et al.* 2012).** The continuous treatment for a longer period of time is highly desirable for depression treatment as the reoccurrence of depressive episodes is high **(Dubovsky *et al.* 2009, Debodinat *et al.* 2010).** To minimize the risk of recurrence, drug treatment for a period of one year is recommended **(Kennedy *et al.* 2009, Demyttenaere *et al.* 2011).**

As per the survey, around 40% patients discontinue the drug treatment within the period of one month while 56% patients shows non-compliance to treatment schedules within 4 months **(Demyttenaere *et al.* 2011).** It is well-known that tolerability and mental problems decline the capability of antidepressants, and that a steady state drug plasma concentration is critical for management of depression **(Serna *et al.* 2010).**

Agomelatine is an antidepressant drug. It is a melatonergic MT_1/MT_2 receptor agonist and it has 5-HT_{2C} receptor antagonist activity. By antagonizing 5-HT_{2C} receptors, it increases noradrenaline and dopamine release specifically in the frontal cortex **(Buoli *et al.* 2014).** A tablet dosage form of AGM is commercially available. The extensive hepatic first-pass metabolism coupled with low biological half-life shows 5% absolute bioavailability on oral administration of AGM **(Debodinat *et al.* 2010).** Due to extensive hepatic first-pass metabolism of drug, a patient on AGM therapy requires a liver function test **(Demyttenaere *et al.* 2011).** For effective treatment of depression, daily medication is required but irregular dose intake may occur due to psychological illness. It can be overcome by development of

transdermal drug delivery system to maintain steady state drug plasma concentration.

Blood-brain barrier (BBB) hinders passage of drug in central nervous system (CNS). BBB is comprised of continuing layer of particular endothelial cells associated with tight junctions. The intricate barrier regulates and restricts systemic delivery of drugs to CNS. Numerous advanced approaches have been discovered to augment passage of drugs through BBB. Nanoparticles are promising carriers for drug delivery to the brain due to distinctive features comprising small size, higher drug solubility, the capability for multi-functionality, and precise drug release profile and potential for targeted drug delivery **(Hersh *et al.* 2016).**

Five layers of skin epidermis from the deepest to superficial are stratum basale also called stratum germinativum, stratum spinosum, stratumgranulosum, stratum lucidum, and stratum corneum. The uppermost layer of skin is stratum corneum and is the physical barrier for passage of drug. Epidermal layer exists below stratum corneum. Epidermis is hydrophobic in nature. Numerous techniques have been developed to increase penetration of drug across skin including the nanoparticulate drug delivery systems ***(*Tomoda *et al.* 2014).**

Polymeric nanoparticles (PNPs) have capability to efficiently penetrate the skin barrier and BBB so as to effectively reach the drug to site of action. Size of PNPs ranges from 1 to 1000 nm. PNPs are able to carry a significant amount of drug across BBB and also provides controlled release profiles. Biodegradable polymers poly (lactic-co-glycolic acid) (PLGA) and poly (lactic acid) (PLA) have been extensively investigated for drug delivery **(Vijayan *et al.* 2013).**

Transdermal drug delivery system (TDDS) is a non-invasive method of drug delivery into systemic circulation by applying it on skin surface. It provides a maximum surface area of 1.73 m^2 and provides constant sink condition. Skin receives one-third of circulating blood at any given time. The drug initially penetrates through the stratum corneum and then passes through the deeper epidermis and dermis without drug accumulation in the dermal layer. When the drug reaches the dermal layer, it becomes available for systemic absorption via the dermal microcirculation. TDDS has many advantages over other conventional routes of drug delivery. It can provide a non-invasive alternative to parenteral routes, thus circumventing issues such as needle phobia. The drugs susceptible to hepatic first-pass metabolism can be effectively administering using transdermal drug delivery system **(Alkilani *et al.* 2015).**

MATERIAL AND METHOD

Materials

Agomelatine (AGM) was received as a gift sample from Mehta API Pvt. Ltd., Mumbai, India. Polymer PLGA (50:50) was supplied as a gift sample by Evonik Degussa India Pvt. Ltd., Mumbai, India. Pluronic F-68 was kindly received as gift sample from Himedia Laboratories Pvt. Ltd., Mumbai, India was used as a stabilizer. Poly vinyl alcohol was received as a gift sample from Himedia Laboratories Pvt. Ltd., Mumbai, India. Ethanol was purchased from Changshu Hongsheng Fine Chemicals Ltd. Propylene glycol was purchased from SRL Chemical Laboratory Pvt. Ltd., Mumbai, India. Transcutol HP was supplied as a gift sample by Gattefosse (France). Oleic acid (OA) was purchase from Loba Chemie Pvt. Ltd., Mumbai, India. N- Methyl-2-Pyrrolidone (NMP) was purchase from S.D. Fine chem Ltd. (Mumbai, India). Isopropyl myristate (IPM) was supplied as a gift sample by Mohini Organics Pvt. Ltd., Mumbai, India. Dimethyl formamide (DMF) was purchased from Ranbaxy Fine Chemicals Ltd.

Method

Preparation of agomelatine polymeric nanoparticles (AGM-PNPs)

Polymeric nanoparticles of drug with polymer were prepared by nano-precipitation method followed by solvent evaporation. The resulting oil in water (o/w) emulsion was formed using different drug: polymer ratio. As shown in table 1, an accurately weighed amount of AGM and PLGA was dissolved in 2 mL mixture of (Acetone1.3 mL+ ethanol 0.7 mL) to form an organic phase (O). It was drop wise added with help of syringe into aqueous phase (W) consisting of Pluronic F-68 %w/v as a stabilizer and then organic solvent was evaporated under continuous magnetic stirring at room temperature for overnight. In the next step, surfactant solution was homogenized using a high-speed homogenizer (IKA Ultra turrex T18, Germany) as shown in figure 1 at speed between 7,000-12,000 rpm followed by probe sonication (Sonics Vibra Cell ™) at 80 % amplitude for 5 minutes. The AGM-PNPs were recovered by centrifugation using a refrigerated centrifuge at 16,000 rpm for 60 min at 4 ℃, washed with distilled water to eliminate or remove additives **(Joshi et al. 2010)**.

The AGM-PNPs pellet obtained after centrifugation was vortexes (Impact, Icon Instruments Company, India) after addition of 5 %w/v mannitol as a cryoprotectant, followed by bath sonication (PCi, India) for 5 minutes and filled in glass vials. The vials were freeze-dried at minus 40 °C and 850 mm/Hg vacuum to obtain a stable dry product. The freeze drying was carried out for 72 hours using a lyophilizer (Mac ®, Macro Scientific Works, India) to obtain a free-flowing AGM-PNPs powder. The product was stored in refrigerator in airtight glass container sealed with parafilm.

The experimental procedure was repeated with the varied drug : polymer ratio and varying concentrations of surfactant. Scale-up experiments were performed to determine large scale application.

Preparation of transdermal patch by a solvent evaporation method using film former machine

Matrix–type transdermal patch containing AGM-PNPs (TP 2) and AGM (TP 1) were prepared by a solvent evaporation method using a film former machine **(Bhalekar et al. 2016).**

Table 1 Preparation of transdermal patch containing AGM-PNPs

Name of ingredients	Formulations	
	TP 1	TP 2
Agomelatine	625 mg	-
AGM-PNPs	-	Weight equivalent to 625 mg drug
Polyvinyl alcohol	250 mg	250 mg
Polyvinyl pyrrolidone -K30	250 mg	250 mg
Polyethylene glycol 400	6 %v/v	6 %v/v
Transcutol-HP	5 %v/v	5 %v/v
Solvent system	33% PG in ethanol (10 mL)	33% PG in ethanol (10 mL)

As shown in table 1, polymers were accurately weighed and dissolved in a specified amount of 33% PG in ethanol (optimized solvent) and allowed to form a uniform dispersion by stirring at 100 rpm for 60 minutes. PEG 400 was added as a plasticizer to obtain flexibility and strength to film. 5% T-HP was used as a penetration enhancer. An accurately weighed amount of AGM and nanoparticles equivalent to 625 mg AGM was added to resultant dispersion of polymer and mixed well using magnetic stirrer. The final dispersion was then spread onto the glass surface of the film former with the help of the dragger. It was allowed to air dry at room temperature. The patches of 2 cm x 2 cm (4 cm^2) were cut and kept in desiccators until further use. The patches containing AGM & AGM-PNPs based patch were prepared with 33% PG in ethanol.

EXPERIMENTAL WORK

Evaluation of AGM-PNPs

Determination of particle size and polydispersity index (PDI)

Photon correlation spectroscopy (PCS) is a technique used to determine the mean particle size diameter and the width of the particle size distribution expressed as PDI. The measurement using PCS is based on the light scattering phenomena in which statistical intensity fluctuations of scattered light from the particles in measuring cell are measured. These fluctuations are due to the random movement of particles in dispersion medium because of the brownian motion of dispersion medium molecules (distilled water).

Zetasizer Nano ZS 90, Malvern Instrument (Malvern, UK) was used to measure the particle size. The instrument was equipped with a laser beam (λ = 633 nm). The scattered light detector is positioned at an angle of 173º. This detection angle is known as the back scatter detection and it has the advantages of improved sensitivity and the possibility of measuring a wide range of sample concentrations. The measuring range of this device is between 0.6 nm to 6 µm. Samples were diluted with double distilled water to an appropriate concentration. The average particle size diameter and PDI are given from at least 30 runs **(Gupta et al, 2010, Wissing et al. 2004).**

Determination of zeta potential

The zeta potential parameter is used to characterize the charge on the surface of the nanoparticles that plays a vital role in determining the stability of the formed nanoparticles. Zetasizer Nano ZS 90 (Malvern Instruments, UK), which calculates the zeta potential by determining the electrophoretic mobility and then applying the henry equation was used to determine zeta potential of the formulations (F1-F9). The electrophoretic mobility is obtained by performing an electrophoresis experiment on the sample and measuring the velocity of particles using laser doppler velocimetry **(Gupta et al, 2010, Wissing et al. 2004).**

Determination of entrapment efficiency

The nanoparticle suspension was subjected to centrifugation at 16,000 rpm for 60 minutes at 4 ℃. The method for determination of entrapment efficiency was based on the amount of AGM recovered from supernatants. It was assumed that the rest of the AGM used during preparation had been encapsulated. The blank used was the supernatant obtained after centrifugation of dummy nanoparticles (without drug) at 10,000 rpm for 30 minutes at 15 ℃. Equation 2 was used to calculate entrapment efficiency **(Elshafeey et al. 2017).**

$$\% EE = \frac{\text{Total drug content} - \text{Amount of free drug in supernatant}}{\text{Total drug content}} \times 100 \quad \text{--- (2)}$$

Characterization of lyophilized AGM-PNPs

The characterization of lyophilized AGM-PNPs was performed using Fourier transform infrared (FT-IR) spectroscopy studies, differential scanning calorimetry (DSC) studies, and X-ray diffraction (XRD) spectroscopy studies.

Fourier transform infrared (FT-IR) spectroscopy studies

The sample of lyophilized AGM-PNPs of optimized formulation (F9) was triturated and mixed well with IR grade potassium bromide in 1:100 ratio. The mixture was introduced in the sample holder of FT-IR instrument and scanned in the range from 4000 to 400 cm^{-1} to obtain the spectrum. The obtained spectrum was compared with the spectrum obtained for AGM and physical mixture of AGM with a PLGA **(Singh *et al.* 2015).**

Differential scanning calorimetry (DSC) studies

The sample of lyophilized AGM-PNPs of optimized formulation (F9) was kept in desiccator for 24 h before thermal analysis. The accurately weighed sample, 5 mg was hermetically sealed in aluminum crucible and heated at a constant rate of 10 ℃/min over a temperature range of 40 to 400 ℃. An inert atmosphere was maintained by purging nitrogen gas at a flow rate of 50 mL/min. An empty aluminum pan was used as a reference **(Singh *et al.* 2015).**

X-ray diffraction (XRD) spectroscopy studies

X-ray diffraction spectrum of lyophilized AGM-PNPs of optimized formulation (F9) was recorded by a diffractogram using Cu-Kα line as a source of radiation at a voltage of 35 Kv and current 25 mA. The sample was measured in the 2θ angle range between 3-80 ^{0} and 0.0053 step size **(Singh *et al.* 2015).**

Surface morphology study of lyophilized AGM-PNPs using scanning electron microscopy (SEM)

The surface morphology of lyophilized AGM-PNPs was visualized using SEM (Zeiss SEM EVO-18, Carl Zeiss Microscopy). The water suspended nanoparticles were mounted on a glass slide as a thin smear and left to dry. The particles on dried glass slide were subjected to gold sputtering and the slide was attached on SEM holder using a double side carbon tape mounted on an aluminum stud. The SEM photomicrographs were captured by operating at an accelerating voltage of 20 kV electron beam at desired magnification **(Vijayan *et al.* 2013).**

Evaluation of transdermal patch

a) Appearance

The transdermal patch formulation TP 1 and TP 2 were visually inspected for color, texture, and homogeneity **(Singh *et al.* 2016).**

b) Average patch thickness

Thickness of transdermal patch formulation TP 1 and TP 2 were measured by using a screw gage micrometer at three different points on the patches. Average values and standard deviation values of three readings were calculated for each transdermal patch formulation TP 1 and TP 2 **(Singh *et al.* 2016).**

c) Weight variation

A set of three patches from transdermal patch formulation TP 1 and TP 2 having an area of 4 cm^2 were weighed on a digital balance and the mean values were calculated. The tests were performed on transdermal patches which were dried at 60 °C for 4 h prior to testing **(Singh *et al.* 2016).**

d) Folding endurance

The test was carried out to check efficiency of plasticizer and strength of patch prepared using different polymers. The folding endurance is defined as the number of folds required to break any polymeric patch. The folding endurance was measured manually by repeatedly folding a small strip of the patch 2 cm × 2 cm (4 cm^2) at the same place until it was broken. The number of times the patch could be folded at the same place without breaking or cracking gave the value of folding endurance. Three patches of each type were taken for the test sample **(Singh *et al.* 2016).**

e) Percent moisture uptake

The percent moisture absorption test was carried out to check the physical stability and integrity of transdermal patch in high humid conditions. The prepared transdermal patches (4 cm^2) were individually weighed accurately and exposed to 85 ± 5% relative humidity in a desiccator containing 100 mL of saturated solution of potassium chloride at room temperature. During this period, the films were weighed at regular time intervals of 24, 48, and 72 h. The percent moisture absorption was determined by using equation 6 **(Singh *et al.* 2016).**

$$\text{Moisture uptake (\%)} = \frac{\text{Final weight of patch} - \text{Initial weight of patch}}{\text{Initial weight of patch}} \times 100 \text{ --- (6)}$$

f) Percentage moisture content

This test was also carried to check the integrity of transdermal patch under dry conditions. The individual transdermal patches (4cm^2) were kept in a desiccator containing fused anhydrous calcium chloride at room temperature. During this period, the transdermal patches were weighed at regular time intervals of 24, 48, and 72 h. The percentage of moisture content was determined by using equation 7 **(Singh *et al.* 2016).**

$$\text{Moisture content (\%)} = \frac{\text{Initial weight of patch} - \text{Final weight of patch}}{\text{Initial weight of patch}} \times 100 \text{ --- (7)}$$

g) Drug content uniformity

The transdermal patch formulation TP 1 and TP 2 were transferred into a graduated glass stopper flask containing 100 mL phosphate buffer saline pH 7.4. The flask was shaken for 24 h in a mechanical shaker followed by bath sonication for 15 minutes. The solution was filtered and 1 mL sample was diluted to 10 mL with phosphate buffer saline pH 7.4. The absorbance was measured at λ_{max} of drug using the placebo patch solution as blank and the drug content was calculated **(Bhalekar *et al.* 2016).**

h) *In-vitro* drug release studies

Franz diffusion cell was employed for *in-vitro* characterization of transdermal formulations. This is a reliable method for the prediction of drug transport across skin from topical formulations. The receptor compartment of the diffusion cell was filled with 20 mL of phosphate buffered saline pH 7.4 contatining 1 %v/v tween 80, and *in-vitro* drug release studies were carried out using synthetic cellophane membrane. The prepared transdermal patches were applied on to the membrane in the donor compartment. The assembly was constantly maintained at 32.0 ± 0.5 °C at 100 rpm. Samples (1.0 mL aliquots) were then withdrawn at suitable time intervals (0, 1, 2, 4, 6, 8, 10, 12, 16, 20, 24, 36, 48 h) and replenished with an amount of medium to maintain the receptor phase volume to 20 mL. The samples were analyzed spectrophotometrically at 277 nm **(Singh *et al.* 2016).**

Release kinetic models

In order to understand the mechanism and kinetics of drug release, the drug release data of the *in-vitro* drug release was analyzed with various kinetic models like zero order, first order, Higuchi, Korsmeyer peppas model and correlation co-

efficient values were calculated for the linear curves by regression analysis of above plots **(Shabbier *et al.* 2017).**

i) *Ex-vivo* skin permeation studies

The *ex-vivo* skin permeation from a transdermal patch formulation TP 1 and TP 2 were studied.

Isolation of skin

Rat abdominal skin was obtained after sacrificing the male Wistar rats. The hair of the abdominal region was removed. Full-thickness skin was surgically removed and the dermis side was wiped with isopropyl alcohol to remove residual adhering fat. The skin was soaked in water at 60 °C for 1 min and washed with water, wrapped in aluminium foil and stored at (minus) 20 °C until used **(Singh *et al.* 2016).**

***Ex-vivo* skin permeation studies**

Ex-vivo skin permeation studies were performed by the Franz diffusion cell with a receptor compartment capacity 20 mL and effective diffusion area 3.14 cm^2. The skin was brought to room temperature by thawing. The skin was hydrated by placing in phosphate buffer saline pH 7.4 with 1 %v/v tween 80 overnight before use and then mounted between the donor and receiver compartment of the Franz diffusion cell, where the stratum corneum side faced the donor compartment. Patches were placed over the skin and covered with paraffin film in order to ensure that the patches do not dislodge from the skin during the test. The receptor compartment of the diffusion cell was filled with phosphate buffer pH 7.4 containing 1 %v/v tween 80. The whole assembly was fixed on a magnetic stirrer, and the solution in the receptor compartment was constantly and continuously stirred using magnetic beads at 100 rpm; the temperature was maintained at 32 ± 0.5°C. The samples were withdrawn at pre-determined time intervals (0, 1, 2, 4, 6, 8, 10, 12, 16, 20, 24, 36 and 48 h) and analyzed for drug content spectrophotometrically at the λ_{max} of the drug. The cumulative amounts of drug permeated per square centimeter of patches were plotted against time. Flux, permeability coefficient & enhancement ratio were calculated by using equation (1), (2) and (3) respectively.

Permeation data analysis

A) The flux (J_{ss}) (mg/cm^2/h) was calculated from the slope of the plot of the cumulative amount of drug permeated per cm^2 of skin at steady state against time using linear regression analysis. **(Haq *et al.* 2018)**

$$\text{Flux } (J_{ss}) \text{ (mg/cm}^2\text{/h)} = \frac{\text{Slope at steady state}}{\text{Effective diffusion area}} \quad \text{--- (1)}$$

B) Permeability coefficient (Kp) were determined by using **(Haq *et al.* 2018).**

$$\text{Permeability (Kp)} = \frac{\text{Flux } (J_{ss})}{\text{Concentration of drug in donor phase}} \quad \text{--- (2)}$$

C) Enhancement ratio (ER) was determined by using **(Haq *et al.* 2018).**

$$\text{Enhancement ratio (ER)} = \frac{\text{Flux with AGM - PNPs based transdermal patch}}{\text{Flux with AGM transdermal patch}} \quad \text{(3)}$$

j) Skin irritation test

The study was performed on the basis of the approval of the Institutional Animal Ethical Committee. The animals (Wistar rats) were grouped and housed in cages, with free excess to standard laboratory diet and water. The dorsal abdominal skin of the rats was shaved carefully avoiding peripheral damage, before 24 h of conducting the study. The transdermal patch was applied onto the nude skin and covered with a non-sensitizing microporous tape. A 0.8 %v/v aqueous solution of formalin was applied as a standard skin irritant. The animals were applied with a new patch each day up to 7 days. The formulation was removed after 7 days; a score of erythema was recorded and was compared with standard. The score of erythema was read and recorded by the Draize scoring method as score 0 for no erythema, score 1 for very slight erythema (light pink), score 2 for well-defined erythema (dark pink), score 3 for moderate to severe erythema (light red), and score 4 for severe erythema (dark red) **(Singh *et al.* 2016).**

k) Animal study

Animal

Male Wistar rats of weight (220 – 250 g) were procured from the central animal facility of UDPS, R.T.M.N.U. Nagpur and used for antidepressant activity of the developed transdermal patch containing AGM-PNPs (TP 2). Animals were kept in plastic cages and had free access to food and water and maintained at proper temperature and humidity. All the experimental protocols were duly approved by the Institutional Animal Ethics Committee (IAEC), UDPS, Nagpur (India). All the experiments were performed in accordance with the guidelines of the Committee for the Purpose of Control and Supervision of Experiments on Animals (CPCSEA), India **(Steru *et al.* 1985; Singh *et al.* 2016; Indulkar 2018)**.

Protocol for the antidepressant study

Male Wistar rats were divided into three groups each containing four rats (n=4). The first group was treated with

saline solution and was considered as control. The second group was treated with AGM tablet oral solution (the 2 mg drug was homogeneously suspended in 1 %w/v solution of hydroxyl ethyl cellulose.) considered as a standard. The third group was treated with a transdermal patch containing AGM-PNPs (2mg).

Tail suspension test

The post-treatment groups of the rats were suspended on the metal rod stand 50 cm above the table top by the adhesive tape placed approximately 1cm from the tip of the tail. Immobility time was recorded during a five minute periods. The rats were observed after a time interval of 1, 2, 6, 12 and 24 h for their immobility time period. Once the experimental time (5 min.) has elapsed, the rats should be returned to the home cage and the tape should be removed from the tail by tenderly pulling it off. The total immobility period were expressed in seconds.

Table 2 Experimental protocol for animal study

Sr. No.	Experimental protocols	Treatments	No. of animals
1	Wistar rats (Control group)	Saline solution	04
2	Wistar rats (Standard group)	AGM Tablet solution (Dose- 2 mg)	04
3	Wistar rats (Test group)	A transdermal patch containing AGM-PNPs (Dose- 2 mg)	04
		Total	n=12

Evaluation

The immobility time period of patch treated animals was compared with normal control and standard groups at different time interval 1, 2, 6, 12 and 24 h.

Stability study

Stability study of transdermal patch formulation TP 2

The transdermal patch formulation TP 2 was selected and the stability studies were carried out at 25 ±2 ºC, 60 ±5 % RH conditions, stored in stability chamber (Remi Instruments Ltd, Mumbai, India). The patches were packed in aluminium foil and kept in above condition for a period of one month. The transdermal patch formulation TP 2 was analysed periodically for drug content and *in-vitro* drug release **(Lalani *et al.* 2012; Katara *et al.* 2017).**

RESULTS AND DISCUSSION

Characterization of AGM-PNPs

Determination of particle size and

The particle size and **polydispersity index** of the AGM-PNPs are important characters in determining the capability of the particles to cross the BBB. The particle size and PDI of all formulations were obtained using Zetasizer Nano ZS 90 and the results are depicted in table 3 and particle size and PDI of optimized formulation are shown in Figure 1.

Table 3 Particle size and PDI of formulations

Sr. no.	Formulation codes	Particle size (nm)	PDI
1	F1	98.4 ± 3.85	0.216 ± 0.02
2	F2	134.2 ± 3.67	0.376 ± 0.01
3	F3	111.5 ± 2.85	0.314 ± 0.06
4	F4	107.1 ± 2.98	0.254 ± 0.02
5	F5	160.5 ± 3.99	0.401 ± 0.04
6	F6	112.3 ± 3.35	0.21 ± 0.03
7	F7	101.2 ± 3.45	0.147 ± 0.06
8	F8	127.3 ± 4.56	0.345 ± 0.04
9	F9	104.5 ± 3.98	0.135 ± 0.02

Table data were expressed as mean ± S.D. (n=3)

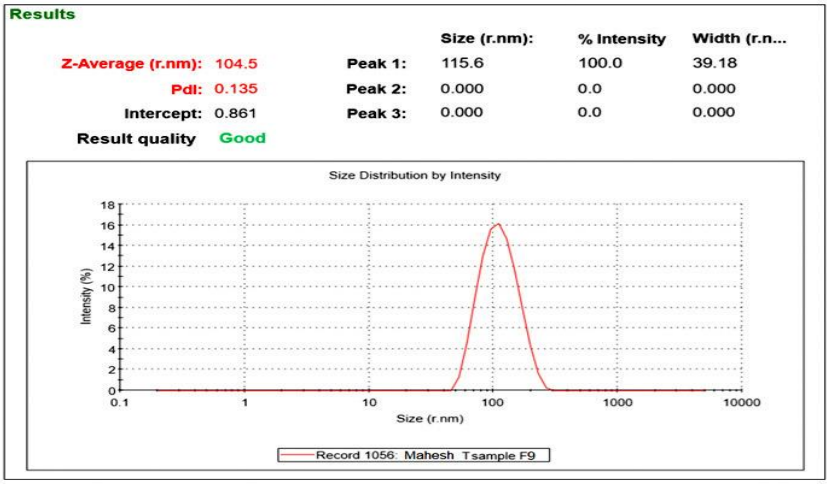

Fig. 1 Particle size and PDI of optimized formulation (F9)

Determination of zeta potential

The zeta potential of the AGM-PNPs is important to determine the stability and uptake mechanism of the particles inside the body. The zeta potential values of formulations are shown in table 4 and zeta potential values of optimized formulation (F9) are shown in figure 2.

Table 4 Zeta potential of formulations

Sr. No.	Formulation codes	Zeta potential (mV)
1	F1	(-) 12 ± 0.52
2	F2	(-) 11 ± 0.67
3	F3	(-) 11.9 ± 0.98
4	F4	(-) 12.1 ± 0.23
5	F5	(-) 10.7 ± 0.39
6	F6	(-) 12.7 ± 0.54
7	F7	(-) 13 ± 0.19
8	F8	(-) 9.1 ± 0.36
9	F9	(-) 13.3 ± 0.46

Table data were expressed as mean ± S.D. (n=3)

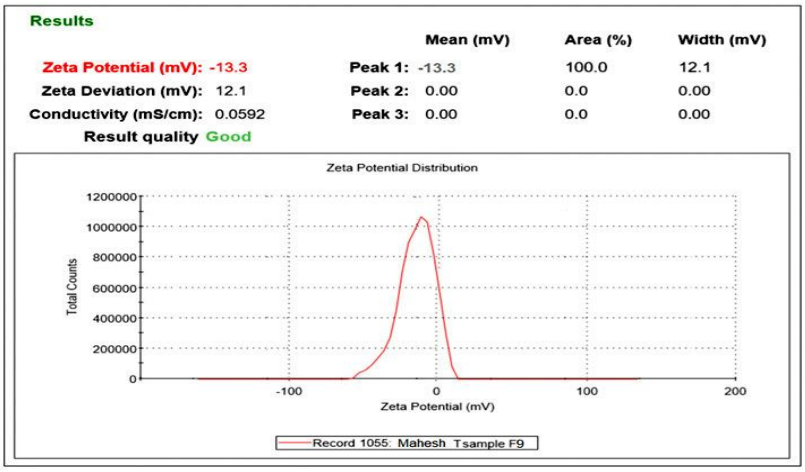

Fig. 2 Zeta potential of optimized formulation (F9)

Determination of percent entrapment efficiency (%EE)

The results of %EE of all formulations are mentioned in table 5.

Table 5 % Entrapment efficiency of all formulations

Sr. No.	Formulation Codes	% EE
1	F1	65 ± 3.36
2	F2	72 ± 4.51
3	F3	70.5 ± 2.26
4	F4	68.3 ± 3.98
5	F5	79.5 ± 4.85
6	F6	84.2 ± 1.19
7	F7	80 ± 2.36
8	F8	69 ± 3.65
9	F9	83.6 ± 4.12

Table data were expressed as mean ± S.D. (n=3)

The particle size (104.5 ±3.98 nm), PDI (0.135 ±0.02), zeta potential (-) 13.3 ±0.48 mV and %EE (83.6 ±4.12%) of the F9 formulation was found to be optimum and thus the formulation F9 was considered as optimized formulation and subjected to further studies.

Characterization of lyophilized AGM-PNPs

Differential scanning calorimetry (DSC) study

The DSC studies for AGM, PLGA polymer and AGM-PNPs were conducted in an inert nitrogen environment. In the DSC studies of AGM, an endotherm at 109.53 ºC with onset at 108.40 ºC and endset at 111.37 ºC was observed (Zhang *et al.* 2018). The enthalpy of endothermic transaction was found to be (minus) 75.24 J/g in case of PLGA polymer a glass transition temperature at 45.86 ºC with onset at 42.76 ºC and end set 48.19 ºC was observed (Kapoor et al. 2015). The enthalpy for glass transition was found to be (minus) 7.26 J/g. The AGM-PNPs prepared using PLGA polymer has shown the first endotherm at 42.12 ºC which was nearer to the value of glass transition temperature of PLGA. The second endotherm was observed at 107.65 ºC with an onset at 88.58 ºC and endset at 105.16 ºC the enthalpy of endothermic transaction was found to be (minus) 4.16 J/g. The second endotherm in DSC thermograph was observed since the drug was made available to the heating process after the polymer has been subjected to the glass transition process. Hence the second endotherm confirmed the melting of AGM. It confirmed preformation of AGM-PNPs. DSC thermograph of AGM, PLGA and AGM-PNPs are shown in figure 3 (a), (b) and (c) respectively.

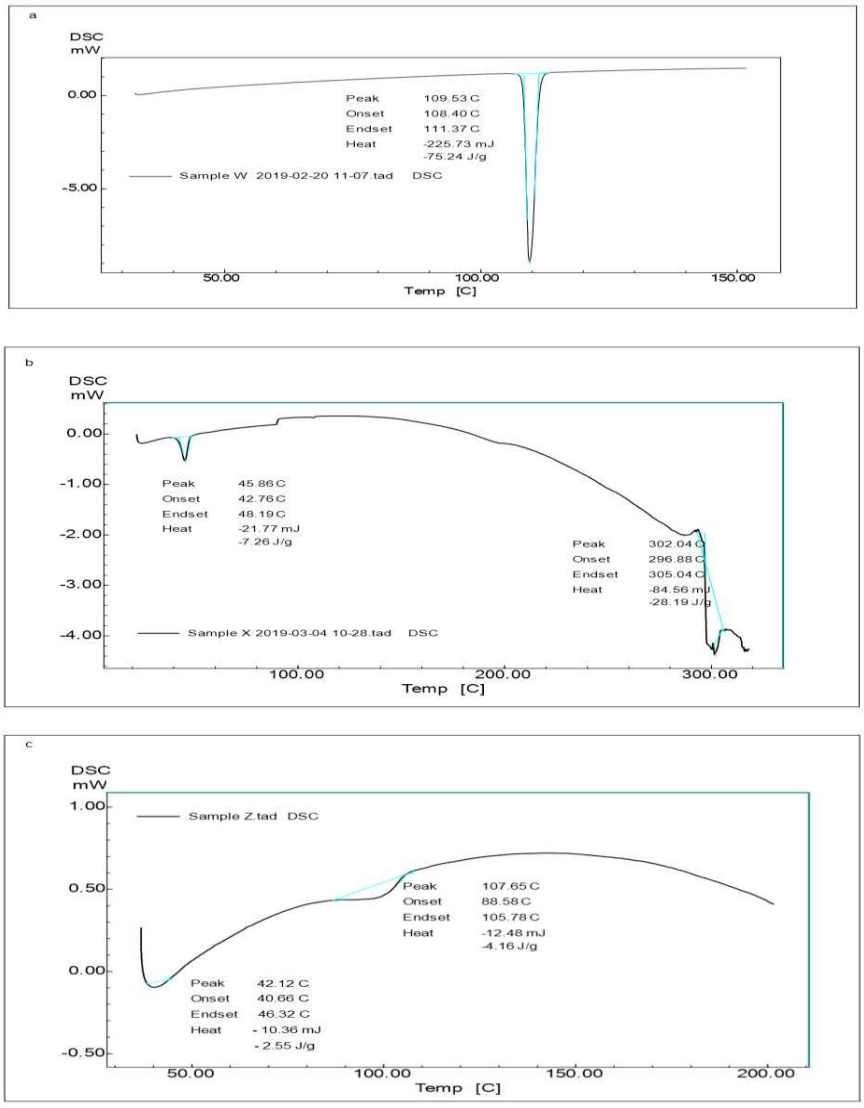

Fig. 3 DSC thermograph of AGM, PLGA and AGM-PNPs **(a)** DSC thermograph of AGM **(b)** DSC thermograph of PLGA **(c)** DSC thermograph of AGM-PNPS

X-ray diffraction (XRD) study

X-ray diffraction spectra of AGM, PLGA polymer and AGM-PNPs are shown in figure 4 (a), (b), (c) respectively. XRD spectrum of AGM has shown crystalline peaks (Zhang et al. 2018). The crystalline peaks were observed at 2θ=6.64, 8.83, 9.40, 10.69, 11.46, 12.76, 13.18, 17.32, 19.14, 20.35, 22.25, 24.38, 25.47 with high intensity. In case of the XRD spectrum of PLGA polymer, a diffused pattern was observed and no single crystalline peak was observed. The amorphous characteristics of PLGA polymer were confirmed **(*Makadia et al.* 2011).** The AGM-PNPs as shown the partial crystalline peaks of AGM and partial diffused pattern of PLGA polymer, but the number of crystalline peaks and their intensity were reduced also the intensity was found to be reduced. It confirmed the adsorption of AGM on the PLGA polymer.

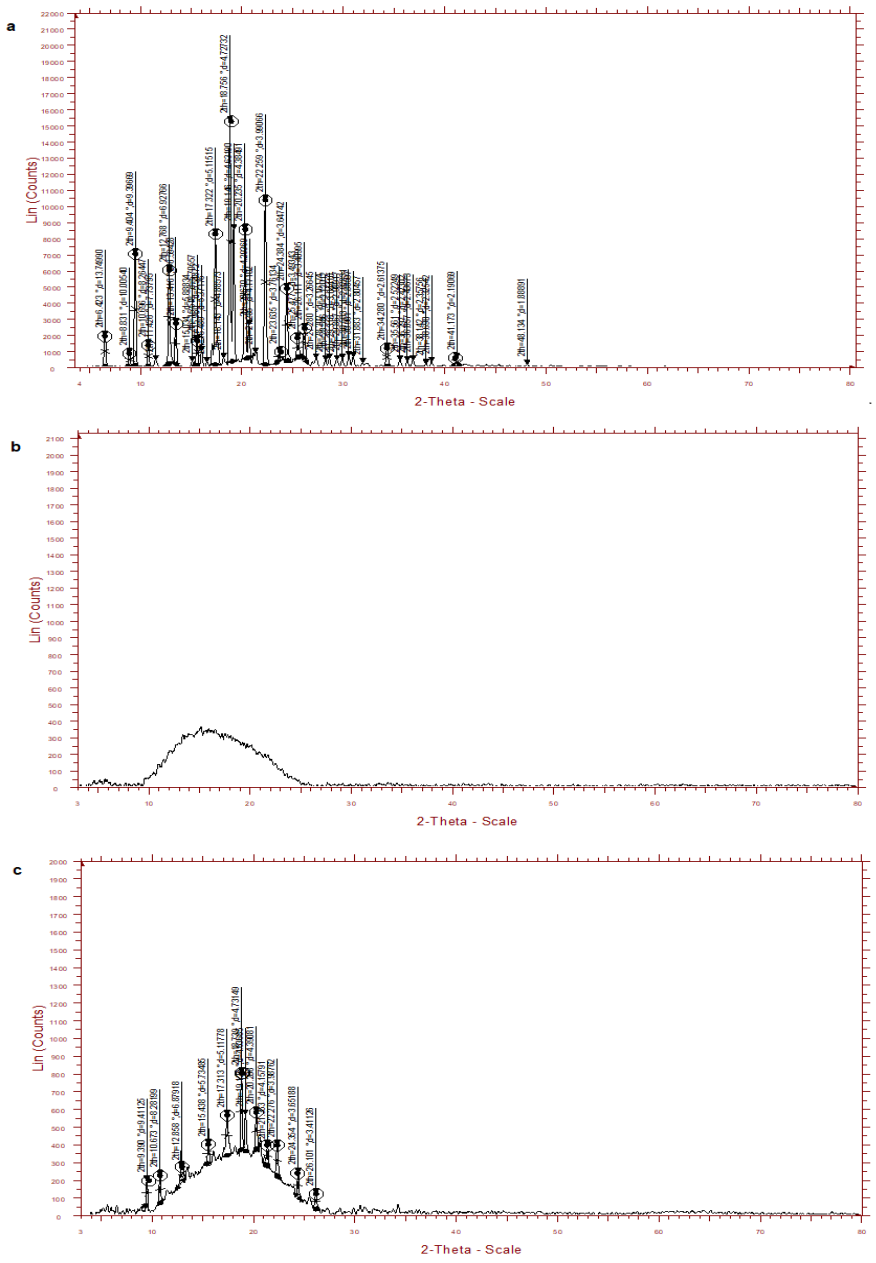

Fig. 4 X-RD spectrum of AGM, PLGA and AGM-PNPs **(a)** X-RD spectrum of AGM **(b)** X-RD spectrum of PLGA **(c)** X-RD spectrum of AGM-PNPs

Fourier transform infrared (FT-IR) spectroscopy study

The FT-IR spectrum of AGM, PLGA and lyophilized AGM-PNPs of optimized formulation (F9) are shown in figure 5 (a), (b), (c) respectively.

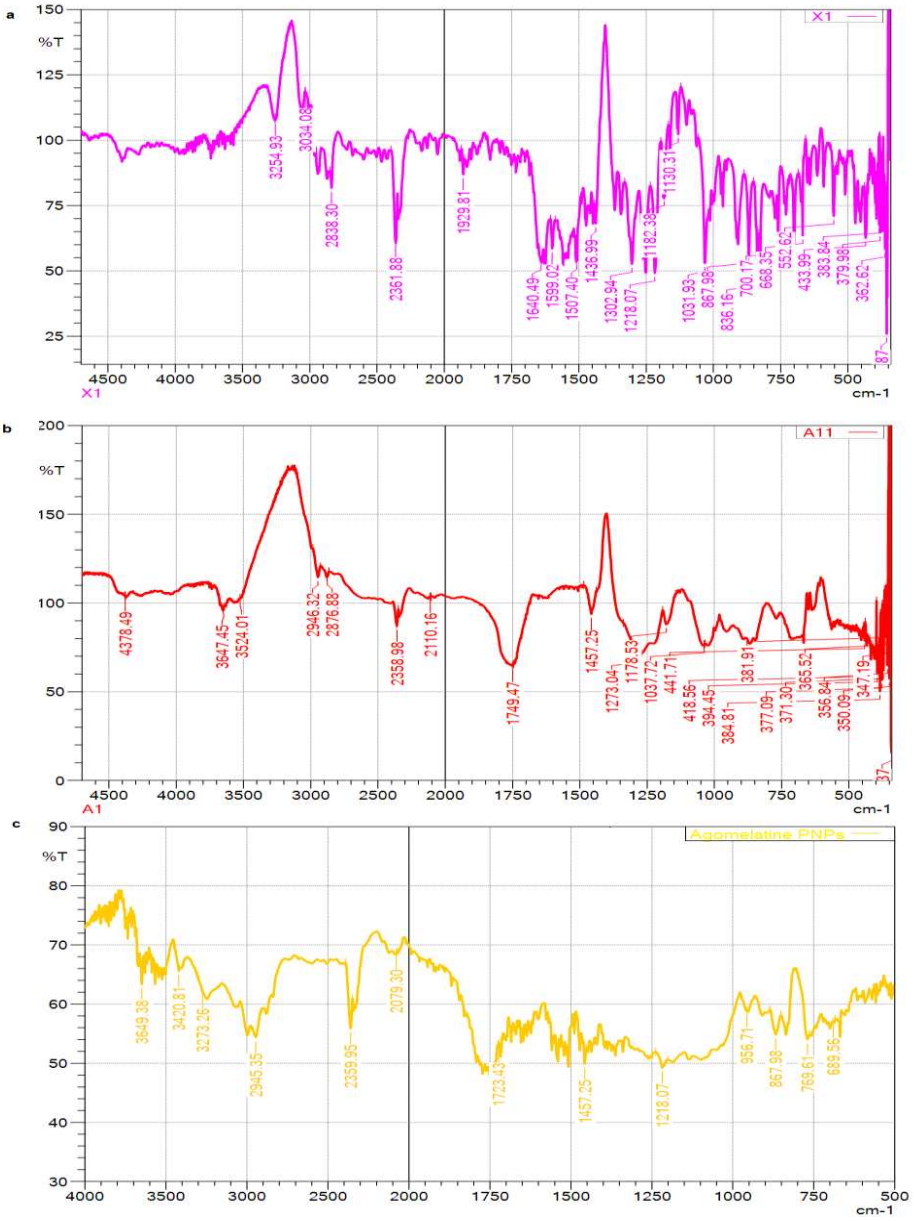

Fig. 5 FT-IR spectrum of AGM, PLGA and AGM-PNPs **(a)** FT-IR spectrum of AGM **(b)** FT-IR spectrum of PLGA **(c)** FT-IR spectrum of AGM-PNPs

The FT-IR spectrums were recorded for AGM, PLGA and lyophilized AGM-PNPs. The FT-IR spectrum of AGM shown stretching vibrations of N-H (3254.93 cm^{-1}), aromatic C-H stretching (3034.8 cm^{-1}), -CH_3 stretching (2838.20 cm^{-1}), the carbonyl stretching vibration of C=O (1640.49 cm^{-1}) and aromatic C=C stretching (1599.02 cm^{-1}) **(Barmpalexis *et al.* 2018).** The FT-IR spectrum of PLGA shown O-H stretching (3647.45 cm^{-1}), C=O stretching (1749.47 cm^{-1}), C-H asymmetric stretching (2946.32 cm^{-1}) and C-O stretching (1273.04 cm^{-1}) (Sousa et al. 2015). The AGM-PNPs has shown the absence of peaks representing the characteristics stretching frequencies of AGM. It concluded that the successfully formation of AGM-PNPs. The characteristics peaks of PLGA were observed in AGM-PNPs, it confirmed the formation of nanoparticles and coating of drug by PLGA polymer.

d) Scanning electron microscopy

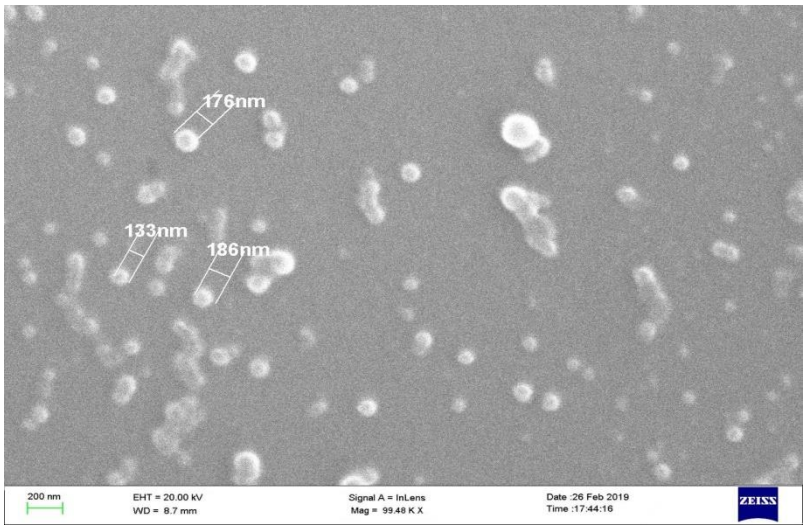

Fig. 6 SEM images of optimized formulation (F9)

The SEM photomicrographs of sample solution (F9 formulation) were obtained and as shown in figure 6. The photomicrographs revealed that the surface was uniform with appearance of spherical shape AGM-PNPs.

Evaluation of transdermal patch containing AGM (TP 1) and transdermal patch containing AGM-PNPs (TP 2)

a) Physical appearance

The transdermal patch formulation TP 1 and TP 2 were evaluated for the appearance (color, texture, and homogeneity) and the results are mentioned in table 6.

Table 6 Physical appearance of transdermal patch formulation TP 1 and TP 2

Formulations	Colour	Texture	Homogeneity
TP 1	transparent	Smooth	Obtained
TP 2	Transparent	Slightly gritty	Obtained

b) Average thickness of transdermal patch

The average thickness of transdermal patch formulation TP 1 and TP 2 were determined and the results are mentioned in table 7.

Table 7 Average thickness of transdermal patch formulation TP 1 and TP 2

Formulations	Thickness (mm)			Average patch thickness (mm)
	Trial I	Trial II	Trial III	
TP 1	0.05	0.06	0.06	0.056 ± 0.005
TP 2	0.07	0.09	0.08	0.08 ± 0.01

Table data were expressed as mean ± S.D. (n=3)

c) Weight variation

Weight variations of transdermal patch formulation TP 1 and TP 2 were determined and the results are mentioned in table 8.

Table 8 Weight variation of transdermal patch formulation TP 1 and TP 2

Formulations	Weight (mg)			Average weight (mg)
	Trial I	Trial II	Trial III	
TP1	36.9	35.1	37.5	36.5 ±1.24
TP2	33.6	36.4	35.2	35.06 ±1.40

Table data were expressed as mean ± S.D. (n=3)

d) Folding endurance

Folding endurance of transdermal patch formulation TP 1 and TP 2 were determined and the results are mentioned in table 9.

Table 9 Folding endurance of transdermal patch formulation TP 1 and TP 2

Formulations	Folding endurance			Average folding endurance
	Trial I	Trial II	Trial III	
TP1	151	160	158	156 ±4.72
TP2	155	169	161	161 ±7.02

Table data were expressed as mean ± S.D. (n=3)

e) Percent moisture uptake

Percent moisture uptakes of transdermal patch formulation TP 1 and TP 2 were determined and the results are mentioned in table 10.

Table 10 Percent moisture uptake transdermal patch formulation TP 1 and TP 2

Formulations	Moisture uptake (%)			Average moisture uptake (%)
	Trial I	Trial II	Trial III	
TP1	1.89	1.61	1.73	1.74 ± 0.14
TP2	1.76	1.98	1.82	1.85 ± 0.113

Table data were expressed as mean ± S.D. (n=3)

f) Percent moisture content

The percent moisture content of transdermal patch formulation TP 1 and TP 2 were determined and the results are mentioned in table 11.

Table 11 Percent moisture content of transdermal patch formulation TP 1 and TP 2

Formulations	Moisture content (%)			Average moisture content (%)
	Trial I	Trial II	Trial III	
TP1	2.16	2.42	1.88	2.15 ± 0.27
TP2	1.97	2.25	2.04	2.08 ± 0.14

Table data were expressed as mean ± S.D. (n=3)

g) Drug content uniformity

Drug content uniformity of transdermal patch formulation TP 1 and TP 2 were determined and the results are mentioned in table 12.

Table 12 Drug content uniformity of transdermal patch formulation TP 1 and TP 2

Formulations	Drug content (mg)			Average drug content (mg)
	Trial I	Trial II	Trial III	
TP1	24.5	24.1	23.8	24.13 ± 0.35
TP2	24.2	24.4	24.7	24.43 ± 0.25

Table data were expressed as mean ± S.D. (n=3)

h) Comparison of *in-vitro* drug release of transdermal patch formulation TP 1 and TP 2

The percent cumulative drug release (% CDR) by *in-vitro* drug release of the transdermal patch with the AGM (TP 1) was compared with that of the transdermal patch with AGM-PNPs (TP 2) as shown in table 13 and illustrated in figure 7.

Table 13 Comparison of *in-vitro* drug release of TP 1 and TP 2

Sr. No.	Time interval (h)	*In-vitro* drug release from the patch formulations (% CDR)	
		TP 1	TP 2
1	0	0	0
2	1	0.49 ± 0.06	0.43 ± 0.05
3	2	0.75 ± 0.04	0.81 ± 0.08
4	4	1.55 ± 0.08	2.88 ± 0.10
5	6	2.84 ± 0.12	6.10 ± 0.23
6	8	5.76 ± 0.56	11.54 ± 0.54
7	10	9.77 ± 1.87	14.59 ± 0.99
8	12	11.84 ± 1.63	21.41 ± 1.45
9	16	22.56 ± 1.11	33.08 ± 1.13
10	20	27.74 ± 1.97	39.31 ± 2.16
11	24	33.98 ± 2.05	50.66 ± 2.36
12	36	42.62 ± 2.26	62.05 ± 1.67
13	48	47.41 ± 1.78	70.16 ± 1.74

Table data were expressed as mean ± S.D. (n=3)

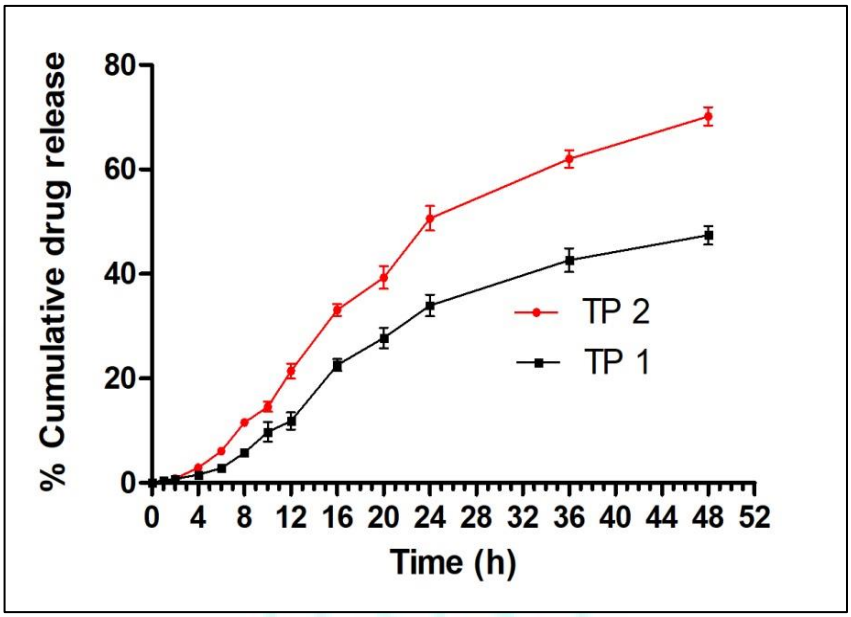

Fig. 7 *In-vitro* drug release plot of transdermal patch formulation TP1 and TP2

Drug release kinetic study

The drug release data of the *in-vitro* drug release study was analysed with various kinetic models like zero order, first order, higuchi model, korsmeyer-peppas model. Coefficient correlation values were calculated for the linear curves by regression analysis of the above plots. The regression coefficient was found to be highest in the korsmeyer-peppas model with the value of R^2= 0.9738 indicating that drug release from the AGM-PNPs followed korsmeyer-peppas model. Results obtained in drug release kinetic studies are given in table 14 and figure 8 (a), (b), (c) and (d) for transdermal patch formulation TP 2.

Table 14 Drug release kinetic studies of *in-vitro* drug release

Sr. No.	Model	R^2 values	
		TP 1	TP 2
1	Zero order	0.9466	0.9536
2	First order	0.9659	0.9672
3	Higuchi	0.9036	0.9216
4	Korsmeyeer- Peppas	**0.9672**	**0.9738**

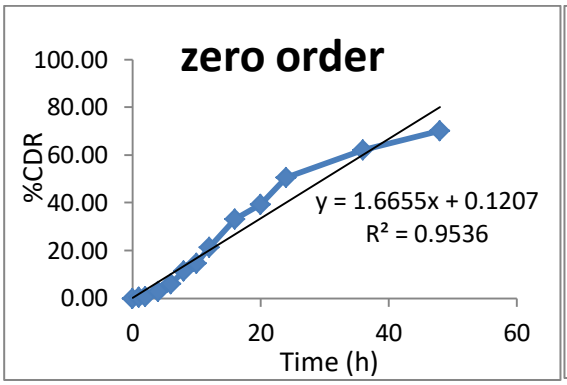

Fig. 8(a) Zero order release kinetic plot

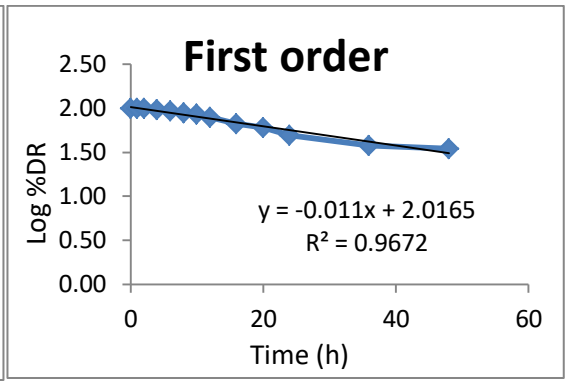

Fig. 8 (b) First order release kinetic plot

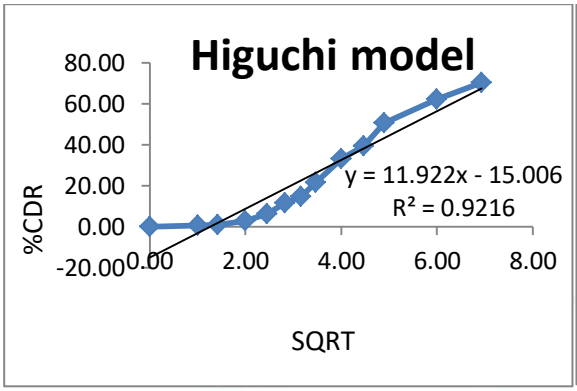

Fig. 8 (c) Higuchi release kinetic plot

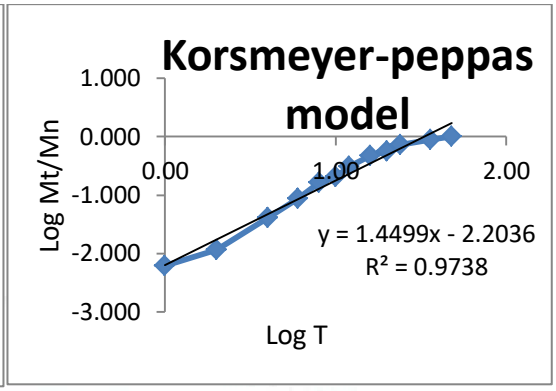

Fig. 8(d) Korsmeyer-Peppas kinetic plot

i) *Ex-vivo* skin permeation studies

The amount of drug permeated (*ex-vivo* skin permeation) of transdermal patch formulation TP 1 and TP 2 was compared and the results are shown in table 15 and illustrated in figure 9. The amount of drug permeated after 24 h from transdermal patch formulation TP 1 and TP 2 was found to be 8.67 mg and 13.66 mg respectively.

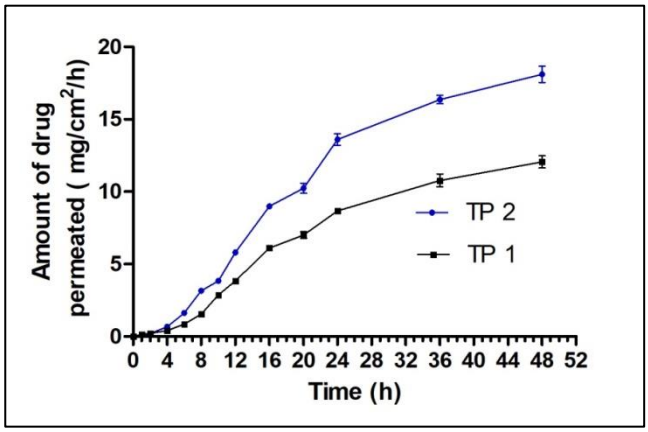

Fig. 9 *Ex-vivo* drug permeation study of transdermal patch formulation TP 1 and TP 2

Table 15 Amount of drug permeated from transdermal patch formulation TP 1 and TP 2 (mg/cm²/h)

Sr. No.	Time Interval (h)		
		TP 1	TP 2
1	0	0	0
2	1	0.13 ± 0.02	0.11 ±0.01
3	2	0.22 ± 0.05	0.21 ± 0.03
4	4	0.40 ± 0.04	0.66 ± 0.02
5	6	0.86 ± 0.09	1.62 ± 0.08
6	8	1.54 ± 0.04	3.15 ± 0.06
7	10	2.86 ± 0.02	3.83 ± 0.03
8	12	3.83 ± 0.08	5.80 ± 0.10
9	16	6.11 ± 0.11	8.98 ± 0.04
10	20	7.01 ± 0.23	10.24 ± 0.35
11	24	8.67 ± 0.12	13.60 ± 0.39
12	36	10.77 ± 0.44	16.36 ± 0.29
13	48	12.05 ± 0.19	18.10 ± 0.15

Table data were expressed as mean ± S.D. (n=3)

Permeation data analysis

The transdermal patch formulation containing AGM-PNPs (TP 2) has shown the least lag time as compared to transdermal patch containing AGM (TP 1) in *ex-vivo* permeation studies is shown in Table 42. The flux values, permeability coefficient and enhancement ratio were found to be enhanced in case of TP 2 as compared to TP 1 is shown in table 16 and table 17 and depicted in figure 10(a) and figure 10(b). It is due to the smallest size of nanoparticles which has high accessibility across the skin.

Table 16 Permeation data analysis of transdermal patch formulation TP 1 and TP 2

Flux (J_{ss}) (µg/cm²/h)		Permeability coefficient (Kp) (cm/h×10³)		Enhancement ratio (ER)	
TP 1	**TP 2**	**TP 1**	**TP 2**	**TP 1**	**TP 2**
131.52 ±2.56	206.05 ± 3.41	5.26	8.24	1	1.57

Table data were expressed as mean ± S.D. (n=3)

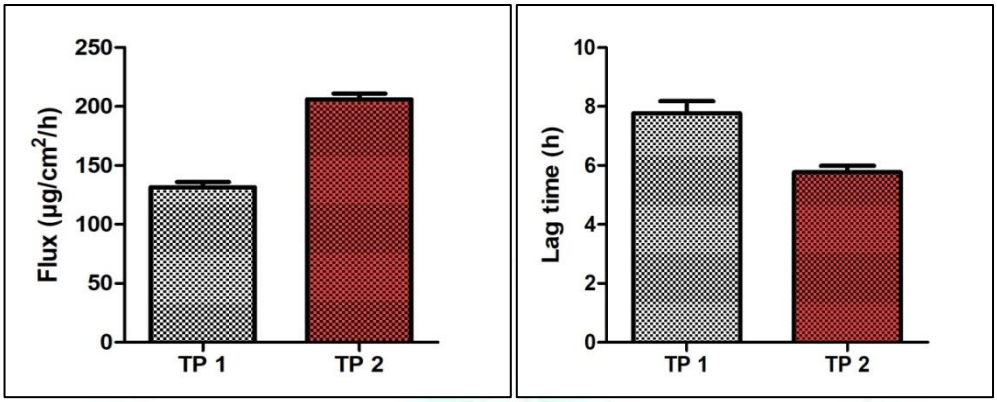

Fig. 10(a) Flux values of TP 1 and TP 2 **(b)** Lag time of TP 1 and TP 2

Table 17 Lag time of transdermal patch formulation TP 1 and TP 2

Lag time (h)	
TP 1	**TP 2**
7.77 ±0.19	5.77 ±0.11

Table data were expressed as mean ± S.D. (n=3)

j) Skin irritation test

Table 18 Results of skin irritation study of the transdermal patch formulation TP 2

Day	Parameter	Standard		Test	
		1	**2**	**1**	**2**
Day 0	Erythema	0	0	0	0
	Edema	0	0	0	0
Day 7	Erythema	3	3	1	1
	Edema	2	3	0	0

The seven-day skin irritation study revealed that test formulation, a transdermal patch formulation TP 2 showed skin irritation score (erythema and edema) of less than 1. From the Draize method of scoring, the standard group (0.8 %v/v formalin solution) of animals showed severe erythema and moderate to slight edema whereas the test animals (transdermal patch formulation TP 2) showed only very slight erythema and no edema on site of application. Results are depicted in figure 11(a), (b), (c) and (d) respectively. According to Draize *et. al 1984*, compounds producing scores of 2 or less are considered non-irritant. Hence, from the study, it was observed that transdermal patch formation TP 2 was non-irritable and safe for therapeutic use.

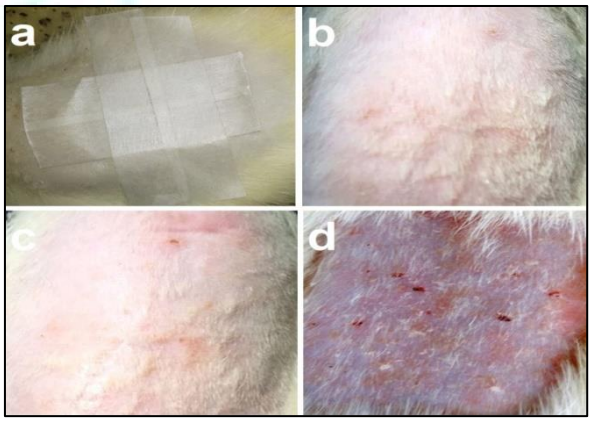

Fig. 11 (a) Transdermal Patch formulation TP 2 application to shaved area, **(b)** Skin of animal on day 0, **(c)** Skin of test group after day 7 of application of TP 2 **(d)** Skin of standard group after day 7

k) Animal study

Tail suspension test (TST)

Table 19 Effect control, treatment and standard group on total immobility time in TST

Treatment group	Total immobility period (Seconds)				
Time interval	**1 h**	**2 h**	**6 h**	**12 h**	**24 h**
Saline solution **(Control)**	155 ± 3.03	157 ± 3.95	151 ± 2.24	153 ± 2.69	150 ± 2.20
Agomelatine tablet oral solution **(Standard)**	141 ± 3.98	105 ± 1.15	139 ± 2.21	151 ± 1.19	148 ± 2.26
Transdermal patch formulation TP 2 **(Test)**	153 ± 2.91	138 ± 21.99	105 ± 2.54	99 ± 3.32	97 ± 2.36

Table data were expressed as mean ± S.D. (n=3)

Above results of tail suspension test revealed that there was a significant reduction in total immobility period over the time interval of 24 h of animals by treating with antidepressant drug AGM. There was a significance difference in total immobility period in control group as compared to a standard group, test group. A transdermal patch formulation TP 2 shows a significant reduction in total immobility period than of oral tablet treatment. The transdermal patch formulation TP 2 shows sustained action over the 24 h and shows a significant reduction in immobility period of animals as compared to standard and control groups. The comparison between the immobility period of control, standard and test at various time interval is shown in table 19 and depicted in figure 12.

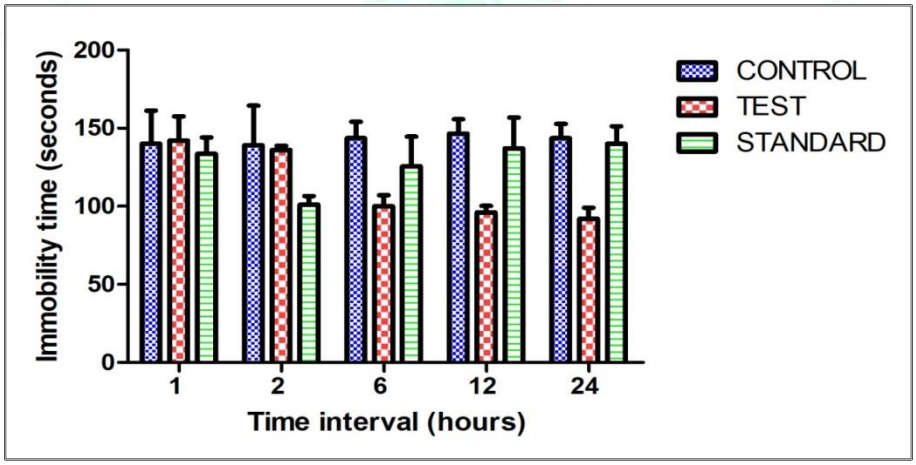

Fig. 12 Effect of control (Saline solution), test (Transdermal patch formulation TP 2) and standard (Oral AGM tablet solution) on immobility time in TST

l) Stability study

The stability study data obtained are given in table 45. The data for *in-vitro* release study is shown in table 20 and graphically depicted in figure 13.

Table 20 Stability study of a transdermal patch formulation TP 2

Time period	Drug content (%)	% cumulative release
	25 ± 2 ºC	**25 ± 2 ºC**
Initial	97.72 ±0.19	71.86 ±1.64
After 1 month	97.45 ±0.26	70.96 ±1.21

Table data were expressed as mean ± S.D. (n=3)

Table 21 Comparison of *in-vitro* drug release of transdermal patch formulation TP 2 initially and after 1 month

Sr. No.	Time interval (h)	*In-vitro* drug release from the transdermal patch formulation TP 2 (% CDR)	
		Initial	After 1 month
1	0	0.00 ±0	0.00 ± 0
2	1	0.40 ± 0.06	0.39 ± 0.03
3	2	0.83 ± 0.09	0.80 ± 0.02
4	4	2.75 ± 0.13	2.78 ± 0.06
5	6	6.19 ± 0.19	6.04 ± 0.21
6	8	12.54 ± 0.61	12.10 ± 0.65
7	10	15.79 ± 0.51	15.01 ± 0.97
8	12	23.24 ± 1.65	22.97 ± 1.32
9	16	32.18 ± 2.12	31.85 ± 0.98
10	20	42.36 ± 1.86	41.20 ±1.65
11	24	51.36 ± 2.01	50.32 ± 1.46
12	36	64.65 ± 1.05	63.30 ± 1.50
13	48	71.86 ± 1.64	70.96 ± 1.21

Table data were expressed as mean ± S.D. (n=3)

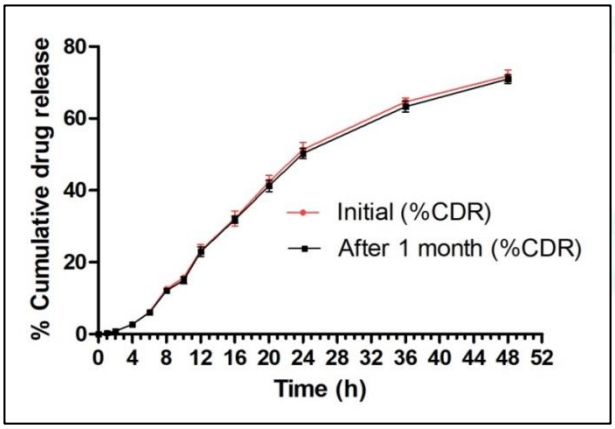

Fig. 13 *In-vitro* release plots of transdermal patch formulation TP 2 stored at 25 ± 2 ºC and 60 ±5 % RH conditions

Stability study of a transdermal patch formulation TP 2 showed that patch was stable and there was no any significant change observed in drug content and % cumulative release at 25 ±2 ºC, 60 ±5 % RH conditions over a period of 1 month.

CONCLUSION

Agomelatine (AGM) is an antidepressant drug. Its extensive hepatic first-pass metabolism coupled with low biological half-life shows 5% absolute bioavailability on oral administration. It can be overcome by development of transdermal drug delivery system to maintain steady state drug plasma concentration.

Blood-brain barrier (BBB) hinders the passage of drug in the central nervous system (CNS). Numerous techniques have been developed to increase penetration of drug across skin including the nanoparticulate drug delivery systems. Polymeric nanoparticles (PNPs) have capability to efficiently penetrate the skin barrier and BBB so as to effectively reach the drug to site of action. Polymeric nanoparticles of drug (AGM-PNPs) with PLGA polymer were prepared by nano-precipitation method followed by solvent evaporation. The particle size, polydispersity index, zeta potential and % entrapment efficiency of the optimized formulation was found to be 104.5 ±3.98 nm, 0.135 ±0.02, (-) 13.3 ±0.48 mV and 83.6 ±4.12% respectively. DSC, FT-IR and XRD methods of instrumental analysis confirmed the formation of AGM-PNPs. In scanning electron microscopy study uniform spherical polymeric nanoparticles were observed.

Matrix–type transdermal patch containing AGM-PNPs (formulation TP 2) and AGM (formulation TP 1) were prepared by a solvent evaporation method using a film former machine. Average folding endurance of transdermal patch formulation TP1 and TP2 were found to be 156 ±4.72 to 161 ±7.02 respectively. Average moisture uptake of transdermal patch formulation TP1 and TP2 were found to be 1.74 ± 0.14 to 1.85 ± 0.113 respectively. Average drug content of formulations TP1 and TP2 was found to be 24.13 ± 0.35 and 24.43 ± 0.25. *In-vitro* drug release from patch formulations TP1 and TP2 were found to be 47.41 ± 1.78 and 70.16 ± 1.74. The drug release data of the *in-vitro* drug release study was analysed with kinetic models zero order, first order, higuchi model, Korsmeyer-peppas model. Regression coefficient was found to be highest for the Korsmeyer-peppas model indicating that drug release from the AGM-PNPs followed Korsmeyer-peppas model. Amount of drug permeated from transdermal patch formulation TP 1 and TP 2 at 48 h was found to be 12.05 ± 0.19 and 18.10 ± 0.15 mg/cm^2/h respectively. In *ex-vivo* skin permeation

studies, transdermal patch formulation containing AGM-PNPs (TP 2) shown least lag time as compared to transdermal patch containing agomelatine (TP 1). Permeability coefficient (Kp) values for formulations TP1 and TP2 were found to be 5.26 and 8.24 (cm/h×10^3) respectively. Enhancement ratio (ER) for formulations TP1 and TP2 were found to be 1 and 1.57 respectively. In the seven-day skin irritation study, transdermal patch as test formulation (TP 2) showed skin irritation score of less than 1. From the Draize method of scoring, the standard group (0.8 %v/v formalin solution) of animals showed severe erythema and moderate to slight edema whereas the test animals (transdermal patch formulation TP 2) showed very slight erythema and no edema on site of application. The results of tail suspension test revealed a significant reduction in total immobility period over time interval of 24 h of animals by treating with agomelatine. A significant difference was observed in total immobility period in control group as compared to a standard group. Transdermal patch formulation TP 2 shown significant reduction in total immobility period than of oral tablet treatment. The transdermal patch formulation TP 2 shown sustained action over the 24 h and a significant reduction in immobility period of animals as compared to standard and control groups. In the Stability study of a transdermal patch, formulation TP 2 was found to be stable and no significant change was observed in drug content and % cumulative release at 25 ±2 ºC, 60 ±5 % RH conditions over a period of 1 month.

REFERENCES

1. Ajazuddin, Alexander A, Dwivedi S, Giri TK, Saraf S, Saraf S, Tripathi DK. Approaches for breaking the barriers of drug permeation through transdermal drug delivery. Journal of Controlled Release 164 (2012) 26-40.
2. Alkilani AZ, MacCrudden MT, Donnelly RF. Transdermal Drug Delivery: Innovative Pharmaceutical Developments Based on Disruption of the Barrier Properties of the stratum corneum. Pharmaceutics.2015 22:7(4):438-70.
3. Begley DJ. Delivery of therapeutic agents to the central nervous system: the problems and the possibilities. Pharmacology and Therapeutics 104 (2004), 29-45.
4. Bhalekar MR., Upadhaya P, Madgulkar A. Solid Lipid Nanoparticles Incorporated Transdermal Patch for Improving the Permeation of Piroxicam. Asian J. Pharm. 10(1) (2016) 45-50.
5. Bommannan D, Potts RO, Guy RH (1991) Examination of the effect of ethanol on human stratum corneum in vivo using infrared spectroscopy. J Controlled. Release. 16, 299-304.
6. Chen Y, Liu L. Modern methods for delivery of drugs across the blood–brain barrier. Advanced Drug Delivery Reviews 64 (2012) 640–665.
7. Crucho CIC, Barros MT, Polymeric nanoparticles: A study on the preparation variables and characterization methods. Materials Science and Engineering C 80 (2017) 771–784.
8. Dhiman S, Singh TG, Rehni AK. Transdermal patches: a recent approch to new drug delivery system. Int J Pharm Pharm Sci, Vol 3, Suppl 5, 26-34.
9. Dominguez A, Suarez-Merino B, Goni-de-Cerio F, Nanoparticles and blood-brain barrier: the key to central nervous system diseases. J Nanosci Nanotechnol. 2014 Jan; 14 (1):766-79.
10. Draize JH, Calvery HO., Methods for the study of irritation and toxicity of substances applied topically to the skin and mucous membranes. J. Pharmacol. Exp. Ther. 82(3) (1944) 377-390.
11. Elmowafy M, Samy M, Abdelaziz AE, Shalaby K, Salama A, Raslan MA, Abdelgawad MA. Polymeric nanoparticles based topical gel of poorly soluble drug: Formulation, ex-vivo and in vivo evaluation. Beni-Suef University Journal of Basic and Applied Sciences. (2017) 6(2):184-191.
12. Elshafeey AH, Fatouh AM, Abdelbary A. Agomelatine-based in situ gels for brain targeting via the nasal route: statistical optimization, in vitro, and in vivo evaluation. Drug Delivery (2017) vol. 24, no. 1, 1077–1085.
13. Gupta H, Aqil M, Khar RK, Ali A, Bhatnagar A, Mittal G. Sparfloxacin-loaded PLGA nanoparticles for sustained ocular drug delivery. Nanomedicine: Nanotechnology, Biology and Medicine 6 (2010) 324-333.
14. Haq A, Michniak KB, Effects of solvents and penetration enhancers on transdermal delivery of thymoquinone: permeability and skin deposition study, Drug Delivery 2018, VOL. 25, NO. 1, 1943–1949.
15. Indulkar P, Prabhavalkar K, Evaluation of the efficacy of combination therapy of agomelatine, duloxetine and sertraline in the management of stress induced depression, IJPSR, 2018; Vol. 9(8): 3210-3222.
16. Jain S, Patel N, Shah MK, Khatri P, Vora N, Recent Advances in Lipid-Based Vesicles and Particulate Carriers for Topical and Transdermal Application, Journal of Pharmaceutical Sciences, (2016) 1-23.
17. Jaiswal J, Poduri R, Panchagnula R. Transdermal delivery of naloxone: ex vivo permeation studies. Int J Pharm. (1999) 179(1):129-34.
18. Jalalpure SS, Joshi SA, Kempwade AA, Peram MR, Fabrication and in-vivo evaluation of lipid nanocarriers based transdermal patch of colchicine, Journal of Drug Delivery Science and Technology, 41 (2017), 444-453.
19. Jalil R, Nixont JR. Microencapsulation using poly (L-lactic acid) 111: Effect of polymer molecular weight on the microcapsule properties. J. MICROENCAPSULATION, 1990, VOL. 7, NO. 1, 41-52.
20. Kapoor DN, Bhatia A, Kaur R, Sharma R, Kaur G, Dhawan S. PLGA: a unique polymer for drug delivery. Ther. Deliv. (2015) 6(1), 41–58.
21. Katara R, Sachdeva S, Majumdar DK, Enhancement of ocular efficacy of aceclofenac using biodegradable PLGA nanoparticles: formulation and characterization, Drug Deliv Transl Res. 2017 Oct;7(5):632-641.
22. Kharat RS, Bathe RS, Formulation and evaluation of transdermal patches of nicardipine hydrochloride, International Journal Of Pharmacy & Technology, June-2016 Vol. 8(2),12609-12628.
23. Lalani J, Rathi M, Lalan M, Misra A, Protein functionalized tramadol-loaded PLGA nanoparticles: preparation, optimization, stability and pharmacodynamic studies, Drug Development and Industrial Pharmacy, 2012: 1–11.
24. Li S. Hydrolytic Degradation Characteristics of Aliphatic Polyesters Derived from Lactic and Glycolic Acids. J Biomed Mater Res. 1999; 48(3):342-53.
25. Lin S, Sharma N, Madan P. Effect of process and formulation variables on the preparation of parenteral paclitaxel-loaded biodegradable polymeric nanoparticles: A co-surfactant study. Asian journal of pharmaceutical sciences 11 (2016) 404–416.
26. Marcus M, Yasamy MT, Ommeren MV, Chisholm D, Saxena S (2012) DEPRESSION: A Global Public Health Concern. https://www.who.int/mental_health/management/depression/who_paper_depression_wfmh_2012.pdf.
27. Mitragotri S, Enhancement of transdermal drug delivery via synergistic action of chemicals, Biochimica et Biophysica Acta, 1788 (2009), 2362–2373.
28. Munoz AS, Guerrero DQ, Vauthier GP, Polymer Nanoparticles for Nanomedicine A guide for their design, preparation and development, Springer, (2016), pp. 87-121.
29. Ostrenga J, Steinmetz C, Poulsen B, Yett S. Significance of vehicle composition: II prediction of optimal vehicle composition. J. Pharm. Sci. 60, (1971) 1180–1183.
30. Pal SL, Jan U, Manna PK, Mohanta GP, Manavalan R. Nanoparticle: An overview of preparation and characterization. Journal of Applied Pharmaceutical Science 01 (2011) (06): 228-234.
31. Panchagnula R, Narishetty STK, Transdermal delivery of zidovudine: effect of terpenes and their mechanism of action, Journal of Controlled Release 95 (2004) 367-379.
32. Panchagnula R, Salve PS, Thomas NS, Jain AK, Ramarao P. Transdermal delivery of naloxone: effect of water, propylene glycol, ethanol and their binary combinations on permeation through rat skin. International Journal of Pharmaceutics 219 (2001) 95–105.
33. Panchagnula, R, Kandavilli S, Nair V, Polymers in transdermal drug delivery systems. Pharmaceutical technology 26(5) (2002) 62-81.

34. Pathan IB, Setty CM, Chemical Penetration Enhancers for Transdermal Drug Delivery Systems, Tropical Journal of Pharmaceutical Research, April 2009; 8 (2): 173-179.
35. Prasanna RA, Anitha P, Chetty CM. Formulation and evaluation of bucco-adhesive tablets of sumatriptan succinate. International Journal of Pharmaceutical Investigation (2011) 1(3) 182-191.
36. R. a. Solutions, Indian Pharmacopoeia 2010. in: M. o. H. a. F. W. Government of India (Ed.), Vol. 1, The Indian Pharmacopoeial Comission, Ghaziabad, 2010.
37. Rang and Dale's Pharmacology. Elsevier Churchill Livingstone, 2012, 7th edition; 553-557.
38. Rao JP, Geckeler KE, Polymer nanoparticles: Preparation techniques and size-control parameters. Progress in Polymer Science 36 (2011) 887–913.
39. Sabliov C, Li J. PLA/PLGA nanoparticles for delivery of drugs across the blood-brain barrier. Nanotechnol Rev 2013; 2(3), 1-17.
40. Saltzman WM, Patel T, Zhou J, Piepmeier JM. Polymeric nanoparticles for drug delivery to the central nervous system, Advanced Drug Delivery Reviews 64 (2012) 701-705.
41. Santos BF, Daflon MP, Chorilli M. Nanotechnology-based drug delivery systems for the treatment of Alzheimer's disease. International Journal of Nanomedicine 2015:10 4981–5003.
42. Sawant KK, Joshi SA, Chavhan SS. Rivastigmine- loaded PLGA and PBCA nanoparticles: Preparation, optimization, characterization, in vitro and pharmacodynamic studies. European Journal of Pharmaceutics and Biopharmaceutics 76 (2010) 189-199.
43. Schimelpfening N, (2018) Most Common Causes of Depression. Verywellmind. https://www.verywellmind.com/common-causes-of-depression-1066772?print
44. Schimelpfening N, (2019) Common Types of Depression. Verywellmind. https://www.verywellmind.com/common-types-of-depression-1067313.
45. Shabbier M, Fazlil AR, Ali S,Raza M, Sharif A, Akhtar MF, Ahmed S, Peerzada S, Younas N, Manzoor I. Effect of hydrophilic and hydrophobic polymer on in vitro dissolution and permeation of bisoprolol fumarate through transdermal patch. Acta Poloniae Pharmaceutica ñ Drug Research, 2017 74 (1) 187-197.
46. Siegel SJ, Makadia HK. Poly Lactic-co-GlycolicAcid(PLGA) as Biodegradable Controlled Drug Delivery Carrier. Polymers 2011, 3, 1377-1397.
47. Singh A, Bali A. Formulation and characterization of transdermal patches for controlled delivery of duloxetine hydrochloride. Journal of Analytical Science and Technology (2016) 7:25.
48. Singh D, Chandra A, Formulation and development of fluoxetine transdermal patches: in vitro and in vivo evaluation, International Journal of Pharmaceutical Research and Innovation, Vol. 9, 2016, 1-8.
49. Singh SK, Hansraj GP, Kumar P. Sumatriptan succinate loaded chitosan solid lipid nanoparticles for enhanced anti- migraine potential. International Journal of Biological Macromolecules 81 (2015) 467-476.
50. Steru L, Chermat R, Thierry B, Simon P, The tail suspension test: A new method for screening antidepressants in mice, Psychopharmacology (1985) 85:367-370.
51. Subedi RK, Seaung YO, Myung KC, Hoo-Kyun C, Recent Advances in Transdermal Drug Delivery. Archives of Pharmaceutical Research 2010; 33(3): 339-351.
52. Suksaeree J, Siripornpinyo P, Chaiprasit S, Formulation, characterization, and in vitro evaluation of transdermal patches for inhibiting crystallization of mefenamic acid, Journal of Drug Delivery, Volume 2017, Article ID 7358042, 1-7.
53. Tanwar H, Sachdeva R. Transdermal drug delivery system: a review. IJPSR, 2016; Vol. 7(6): 2274-2290.
54. Tiruwa R, A review on nanoparticles – preparation and evaluation parameters. Indian J. Pharm. Biol. Res. 2015; 4(2):27-31.
55. Tripathi KD. Essentials of Medical Pharmacology, 6th edition, Jaypee Brothers Publishing House Pvt. Ltd. Reprint; 2009:476-556.
56. Vakadapudi ABS, Gummidi B, Thamrapalli S, Effect of additives and solvents on inhibition of crystallization in transdermal patches containing repaglinide, International Journal of Pharma Sciences and Research, Vol 5 (02) 2014, 25-30.
57. Vijayan V, Reddy KR, Sakthivel S, Swetha C. Optimization and Characterization of repaglinide biodegradable polymeric nanoparticle loaded transdermal patchs: In vitro and in vivo studies. Colloids and Surfaces B: Biointerfaces 111 (2013) 150-155.
58. Wang Y, Zhang H, Pu C, Wang Q, Tan X, Gou J, He H, Zhang Y, Yin T, Tang X. Physicochemical Characterization and Pharmacokinetics of Agomelatine-Loaded PLGA Microspheres for Intramuscular Injection. Pharm Res (2019) 36:9.
59. Williams AC, Barry BW, Penetration enhancers, Advanced Drug Delivery Reviews, 56 (2004) 603–618.
60. Wissing SA, Muller RH, Manthei L, Mayer C, Structural characterization of Q10-loaded solid lipid nanoparticles by NMR spectroscopy, Pharmaceutical Research, Vol. 21, No. 3 (2004) 400-405.
61. Yadav SC, Kumari A, Yadav SK, Biodegradable polymeric nanoparticles based drug delivery systems. Colloids and Surfaces B: Biointerfaces 75 (2010) 1–18.
62. Yadav V, Altaf bhai S, Mamatha M, Prasanth Y. Transdermal drug delivery: A technical writeup. Journal of Pharmaceutical and Scientific Innovation 1 (1), 2018, 5-12.
63. Zhou Y, Peng Z, Seven ES, Leblanc RM, Crossing the blood-brain barrier with nanoparticles, J Control Release. 2018 Jan 28;270: 290-303.